JOURNAL OF SPACECRAFT AND ROCKETS
Vol. 35, No. 3, May–June 1998

Particle-in-Cell Code Analysis of Charging Hazards and Wake Studies Experiment

Gregory B. Giffin,* Daniel E. Hastings,† Gabriel I. Font,‡ and Graeme B. Shaw*
Massachusetts Institute of Technology, Cambridge, Massachusetts 02139
and
David L. Cooke§
U.S. Air Force Phillips Laboratory, Hanscom Air Force Base, Massachusetts 01731

The Charging Hazards and Wake Studies (CHAWS) experiment characterized the ion current collection to a negatively biased Langmuir probe mounted in the wake of the Wake Shield Facility (WSF) during the STS-60 and STS-69 (CHAWS I and II) missions. A three-dimensional particle-in-cell code is applied in analysis of the three data categories: high-voltage wake ($>|\sim 100$ V|), low-voltage wake ($<|\sim 100$ V|), and data obtained when the shield was inverted and the probe pointing into the plasma flow (ram-oriented data). The high-voltage analysis finds that the code underpredicts the data by about a factor of two when the code inputs are the detector measurement of plasma density and ion temperature, assuming that all of the plasma ions were O^+ and assuming that the electron temperature was 1.5 times the ion temperature. Analysis in the other two categories allowed identification of the input error. The low-voltage analysis rules out low Mach number flow, which contributes disproportionately to the current, demonstrating that it was composed of H^+ (rather than ionized contamination from the Shuttle/WSF or turbulent O^+) and not present in quantities significant enough to invalidate the all O^+ assumption of the code. The ram-oriented data analysis, in conjunction with space charge limited collection theory and International Reference on the Ionosphere, 1990 version (IRI-90), prediction, suggests that the CHAWS detectors underestimated the ambient plasma density and thereby reconciles the high-voltage code–data comparison. Other significant findings of this work include location of O^+ collection turn-on voltages, the possibility that electron heating ($T_e \sim 5T_i$) occurred in the ram direction, and the code demonstration of wake-side collection insensitivity to T_e, confirming its orbit motion limited nature.

Nomenclature

e = electron charge
I = current
j_i = ion current density
j_0 = ram current density
k = Boltzmann's constant
l_p, r_p = probe dimensions
M_n = normal Mach number
n_∞ = plasma density
T = electron temperature
v_0 = orbital velocity
ε = ion–electron temperature ratio
ε_0 = permittivity of free space
θ = angle of attack
λ_D = ambient debye length
ξ = debye ratio
σ = charge density
Φ_p = probe potential
ϕ = electric potential

Introduction

THE need to design for the interaction between spacecraft operating in low Earth orbit (LEO) and the plasma environment has been recognized since the advent of space flight. The issue has received additional attention in recent years inasmuch as charging phenomena may be enhanced by increases in spacecraft size and power.[1] In mild cases, isolated surfaces can attain significant potentials relative to the plasma, altering the response characteristics of detectors and complicating scientific investigation. In more severe cases, there may be electrical discharge between isolated surfaces or nearby objects. This arcing may have a wide variety of detrimental effects including damage of critical electronics, electromagnetic noise, surface erosion, and structural damage. Spacecraft surface charging has been linked directly to anomalous behavior of some satellites[2] and implicated in the total loss of others.[3]

One of the least understood and difficult aspects of spacecraft charging has been interactions occurring on the wake side of vehicles. In LEO the flow around an orbiting object is mesothermal. That is, the electron thermal velocity is much greater than that of the spacecraft while the ion thermal velocity is much less. The mesothermal flow causes formation of the wake, a region behind the spacecraft that is essentially devoid of ions but populated by electrons with a reduced density in equilibrium with their own space charge (Fig. 1, from Ref. 4).

Electrically isolated surfaces or objects within a wake become negatively charged with respect to other spacecraft components due to the lack of ions. Under nonauroral electron conditions, the charging is typically a few electron volts, whereas in the polar auroral electron environment, this charging can be much greater and, therefore, more threatening. Wake charging can also be more pronounced and, correspondingly, more dangerous when objects operating at significant voltage levels, such as power supplies or transmission wires, are present. In addition, ion current collection by negatively biased power supplies or uninsulated wires would act as a parasitic current and would reduce the overall efficiency of the power system.

Previous work on LEO spacecraft wake charging interaction has consisted of numerical simulation[5–7] and laboratory work[4,8] but prior to the Charging Hazards and Wake Studies (CHAWS)[9] there had been insufficient in situ data[10,11] available to verify the validity of those investigations. The CHAWS experiment was designed to achieve the following objectives.

Received June 16, 1997; revision received Dec. 1, 1997; accepted for publication Dec. 30, 1997.

*Research Assistant, Aeronautics and Astronautics Department, Space Systems Laboratory, Room 37-438, 77 Massachusetts Avenue.
†Professor, Aeronautics and Astronautics Department, Space Systems Laboratory, Room 37-438, 77 Massachusetts Avenue. Associate Fellow AIAA.
‡Postdoctoral Associate, Aeronautics and Astronautics Department, Space Systems Laboratory, Room 37-438, 77 Massachusetts Avenue. Member AIAA.
§Geophysicist.

Table 1 Summary CHAWS I and II data

Parameter	CHAWS I Grappled High V	CHAWS II WSF free flight Low V	CHAWS II WSF free flight High V	CHAWS II WSF grappled Low V	CHAWS II WSF grappled High V	CHAWS II Ram
I-V sweeps	8	4	12	12	27	4
n_∞, 10^{10} m^{-3}	1.7–61	7.3–29	5.3–7.8	2.3–41	2.3–32	~6 to ~20[a]
kT_i, eV	0.08–0.14	0.05–0.08	0.06–0.13	0.03–0.13	0.04–0.14	~0.1[a]
θ, deg	−28 to −2.0	−4.5–3.8	−4.6–2.6	−40.4–2.4	−41.1–39.4	Ram oriented

[a]Values were not measured but determined indirectly from analysis.

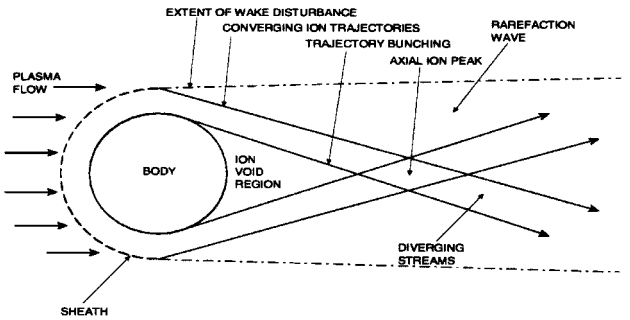

Fig. 1 Basic wake characteristics.[4]

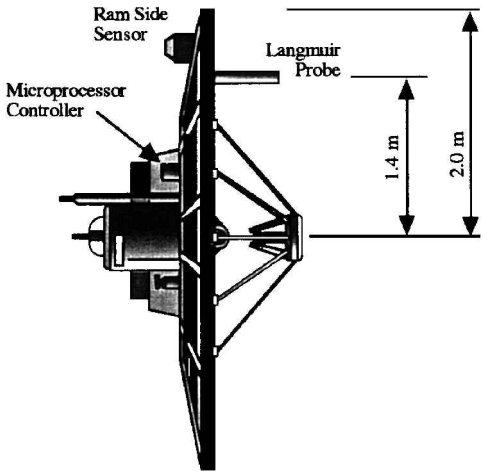

Fig. 2 CHAWS components mounted on the WSF.

1) Flight test a new generation of miniaturized particle detectors by using them to measure the ambient low-energy ion population on the ram and wake side of the Wake Shield Facility (WSF).

2) Determine and understand the current–voltage characteristic of a negatively biased object in a plasma wake under a variety of environmental conditions.

3) Compare the results to preflight and postflight numerical simulation.

4) Derive a general, i.e., applicable to geometries other than CHAWS, analytical model consistent with both the data and the simulation from which future spacecraft may be designed to avoid hazards posed by wake charging.

This paper presents results that contribute to the second objective and satisfy the third. It compares the particle-in-cell (PIC) code simulation results to the observed probe I-V (current–voltage) characteristic data in three distinct ion collection regimes: the low-voltage (H^+) ion collection, the high-voltage frontal stream (O^+) ion collection, and the ram-oriented ion collection. These comparisons allow a greater understanding of the CHAWS current–voltage characteristic and form the foundation for a later work,[12] which addresses the fourth objective.

CHAWS Experiment

The CHAWS experiment[9] was designed by the U.S. Air Force Phillips Laboratory at Hanscom Air Force Base, Massachusetts, and was flown to study the interaction between the WSF and its wake environment. The position of various CHAWS components on the WSF is shown in Fig. 2. The WSF is a self-contained spacecraft, with limited cold gas propulsion for separation from the Shuttle after release from the robotic arm. Separation from the Shuttle of 70 miles was desirable to avoid contamination from the Shuttle environment. During STS-60 CHAWS data were obtained with the WSF mounted on the Shuttle arm whereas on STS-69 data were obtained for both the mounted and the free flying modes.

CHAWS studied the wake environment by recording the positive ion collection to a highly biased negative probe mounted on the back of the shield while simultaneously observing the ion temperature and density with retarding potential analyzer (RPA) sensors mounted on the ram side. The RPAs also measured the WSF floating potential and found it to be only a few volts. The angle that the shield made with the plasma flow was recorded by the Orbiter when attached to the arm and by the WSF attitude control system when in free flight. The angle of attack is considered negative if the probe is tilted toward the plasma flow.

The probe consisted of a grounded central structure and a stainless steel outer shell. It had a length of 0.45 m and a radius of 0.05 m. The bias application was broken down into eight predefined sweeps of voltage ranges from 0 to −31, −62, −325, −775, −1550, −2325, −3100, or −4825 V. Each sweep had 32 points. A full voltage sweep took 1 min, during which each of the ram-side sensors made eight measurements of the plasma ion density and temperature.

CHAWS Results

The separation voltage between the high- and the low-voltage wake ion collection regimes is referred to as the turn-on voltage. At voltages below turn-on, the collection is limited to ions that can enter the wake unassisted by the attractive potential, which does not significantly extend beyond the edge of the WSF. Above the turn-on voltage, however, the potential begins to draw in ions directly from the stream and should quickly overwhelm the current due to ions that enter the wake unassisted. A brief overview of each CHAWS flight has been presented[13] and a summary of the observations obtained is included as Table 1. Another reference[14] presents the complete set of sweeps and the measured ambient plasma parameters from STS-69. The ion density and temperature could not be measured by the ram-side sensor when the shield was inverted because the sensor was no longer exposed to the plasma flow. Actual I-V measurements are presented along with PIC comparison and analysis in the following sections.

PIC Code

The essential problem addressed by the PIC code[15] was the computation of the electric potential from the charge density via the Poisson equation

$$(1/\varepsilon_0)\nabla^2\phi = \sigma \tag{1}$$

The density was weighted onto the grid node points using a linear interpolation method. The solution to the potential distribution was found with a three-dimensional alternating direction implicit (ADI) explicit scheme. The field was then found by differentiating the potential and back interpolating the result to the particles. The particle velocities and positions were then updated through a time-centered leap-frog scheme, which maintained second-order accuracy.

The computational geometry of the WSF is provided in Fig. 3 (one of the results). Much of the apparatus seen in Fig. 2 has been removed as it is mostly conducting and grounded to the WSF. The

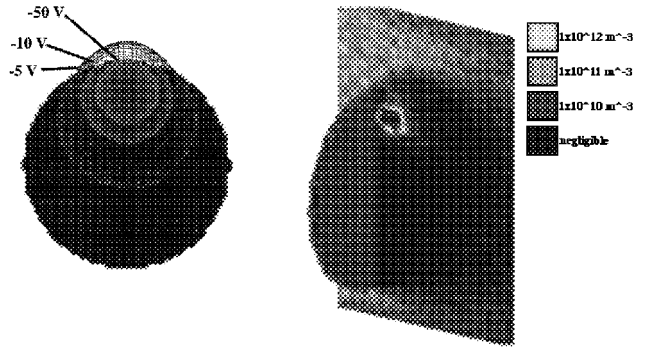

Fig. 3 Centerline potential contour cross section for $\Phi_p = -1500$ V (left) and O^+ centerline density cross section for $\Phi_p = -1500$ V (right). The potential extending into the frontal stream is in tens of volts.

computational grid was Cartesian, and the node points were equally spaced in all directions. Cell spacing was $L \cdot \lambda_D$ where L is less than 10 and λ_D is the ram-side ambient debye length. The electrons were treated as a Boltzmann fluid and were assumed to be in equilibrium with the potential. The simulation was 50 cells in size along the WSF normal and 75 cells in the other dimensions. The flow entrance was located one-third of a body radius in front of the WSF, whereas the side boundary near the probe was one body radius above the top edge of the shield. The exit plane was one body radius behind the shield, whereas the other side boundaries were each one-third of a body radius from the edge of the WSF. These and the other boundaries were chosen through trial and error until alteration did not affect the simulation results. All boundaries and surfaces were assumed to be fully absorbent.

The particles were loaded randomly in space with a Maxwellian distribution of velocities. The orbital velocity of the WSF was then superimposed onto the distribution. The simulation was run for one convective time period to allow the flowfield to become established. Another time period was then allowed to run, and the ion current was taken as the average of each timestep result. Trial runs determined that a minimum of 5 superparticles per ram-side cell and a maximum timestep of 0.1 times the ion plasma frequency were required to avoid altering simulation results. The probe potential was held fixed for a given simulation and measured with respect to the plasma. The shield potential, typically a few volts negative with no observed artificial fluctuations, was adjusted at each timestep by observing the flux to its surface and enforcing the zero net current. A total of 1.5×10^6 superparticles was used, and the simulation took approximately 2 days on an SGI Workstation with 256 Mbytes of available RAM to obtain one data point. The code found no evidence of temporal instability for the ions.

High-Voltage Ion Wake-Side Collection Simulation and Analysis

For the high-voltage PIC simulation it was assumed that the plasma flow was composed solely of O^+ ions. One sweep from each of CHAWS I and II was chosen for simulation. The simulation parameters and those of the actual data are provided in Table 2.

The expansion of the electric potential contours is shown in Fig. 3 for a Φ_P of -1500 V under the sweep 10 simulation parameters. The contours spread out behind the shield and below the probe. Above the probe, the contours are more confined and spread out less as the space charge of the frontal stream is contacted. Nevertheless, the contours expanding into the stream are in the negative tens of volts. The central plane cross section of the ion density, also included in Fig. 3, demonstrates that at the lower edge of the shield there is the expected Mach expansion of ions. However, the upper edge has a crescent-shaped area that is cleared of ions. The ions that enter the crescent area are diverted from the frontal stream into the wake and impact the WSF, as shown in Fig. 4. The lighter gray area below the probe on the rear of the wake shield is an area where the incident ion flux is about half that of the ram-side ion flux. The white areas on the probe correspond to an incident flux of about five times the ion flux. The sample trajectories, which all begin in the plane of the shield in different locations, all converge at nearly the same point.

Table 2 Simulation and actual sweep parameters

Parameter	n_∞, m^{-3}	T_i, eV	θ, deg	T_e, eV	v_0, m/s
Code	1.0×10^{11}	0.10	0	$1.5T_i$	7600
Sweep 10	1.0×10^{11}	0.10	-10		7600
Code	1.5×10^{11}	0.09	0	$1.5T_i$	7600
Sweep 68	1.5×10^{11}	0.09	1.7		7600

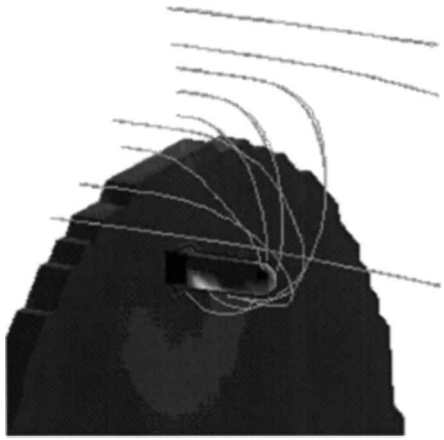

Fig. 4 Sample O^+ ion collection trajectories for a Φ_P of -1500 V.

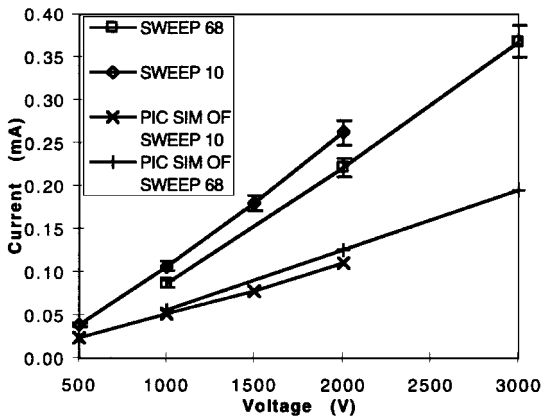

Fig. 5 Comparison of PIC predicted current to CHAWS data.

A comparison of the total simulated probe current to both CHAWS I and II data is provided in Fig. 5. The data have been corrected for the estimated amount of secondary electron emission current.[12] Both the simulation and the flight results are linear, but the simulation underestimates the data by about a factor of two.

The factor of roughly two difference between the code and the data is surprising. Possibilities for this discrepancy include 1) systematic code error, 2) incorrect or inaccurate inputs to the code, 3) an additional source of current that is present in the data but is not accounted for in the code, or 4) error in the data. The WSF floating potential was generally only a few volts relative to the plasma and is, hence, not considered a plausible explanation.

A systematic error in the code is unlikely. Another simulation code, POLAR,[16] developed by the U.S. Air Force Phillips Laboratory, was designed to model the interaction of spacecraft with LEO plasma. POLAR is a three-dimensional steady-state Poisson–Vlasov solver and is, therefore, different from codes based on PIC methodology. POLAR was used to both to design the CHAWS experiment and to perform preflight predictions. Comparison between POLAR and the PIC code used has demonstrated that the two codes yielded identical current–voltage prediction for the same set of input parameters.[17] That each code would possess the same systematic error is improbable.

The other possible sources of error are uncertainty in the data or uncertainty in the assumptions. These error possibilities include electron temperature, ion density, and low Mach number plasma components. The ion temperature has an estimated error of about

±30%, and the maximum impact this should have on the collected current is about ±15% (Ref. 12).

The electron temperature was not measured in the experiment. Space charge limited current collection can, in general, be quite sensitive to the electron–ion temperature ratio.[18] In addition, other investigations[19,20] have noted an increase in the electron temperature within the wake of a spacecraft and place this ratio as high as three times the 1.5 ratio used in the simulation results of Fig. 5. Code runs for higher ratios, however, found that even at $T_e = 5T_i$ the collected current only increased by ~10%. Hence, an error in our electron temperature assumption is not sufficient to explain the code–data difference. The insensitivity of the current collection to the electron temperature is also confirmation of the finding[12] that the high-voltage wake-side collection is orbit motion limited in nature. The next section examines the possible contribution by low Mach number flow components, and the section following that examines possible error in the ion density measurement.

Low Voltage (Preturn-On) Wake-Side Ion Collection

Determination of the ion flux to wake-side surfaces is a difficult problem. For the purpose of this discussion, it is sufficient to employ the assumption that the ions are neutral. The flux to a wake-side surface is then given by

$$j_i = j_0\left[e^{-M_n^2} + M_n\sqrt{\pi}(1 + \mathrm{erf}(M_n))\right] \approx j_0 e^{-M_n^2} \qquad (2)$$

The approximation is good for wake-side surfaces when $M_n \geq 5$ or so. The Mach number is defined here as the spacecraft orbital velocity normalized by the ion thermal velocity. Although the electron space charge will draw ions into the wake, Katz and Parks[1] have shown that the neutral approximation is quite good. Therefore, Eq. (2) demonstrates that in the low-voltage ion collection regime any measurable collection to the probe should consist almost exclusively of low Mach number flow ions. One possibility for the code–data discrepancy in the high-voltage analysis of the preceding section is the significant contribution to the current by low Mach number flow that more readily enters the wake environment. Simulation of the low-voltage ion collection should provide insight into whether low Mach number flow is a significant component of the observed high-voltage current collection.

H^+ is the most promising possibility for the low Mach number flow composition. Ionized Shuttle contamination is ruled out because the low-voltage I-V and ram-side sensor measurements did not vary with whether the WSF was attached to the remote manipulator system (RMS) or free flying several miles from the orbiter. Turbulent O^+, although it may be responsible for the noiselike fluctuations in the ram-side sensor readings,[9] is also ruled out because it should not be sufficiently slowed to pass the restriction set by Eq. (2). H^+, by virtue of its lower mass, possesses a Mach number one-quarter that of the dominant O^+ species. For typical LEO ion temperatures, Eq. (2) predicts that about one-fifth of the ram flux of H^+ ($M \sim 1.25$) may impact the rear of the WSF whereas practically none of the O^+ ($M \sim 5$) atoms would be able to do the same. The amount of LEO H^+ at ~300 km as a percentage of the total ambient ion density at typical Shuttle altitudes has been quoted as anything from 0.1% (Ref. 21) to 30% [International Reference on the Ionosphere, 1990 version (IRI-90)]. An H^+ signal was not observed in the ram-side sensor readings[13] and indicates that the H^+ density was below about 10%.

Previous work using Dynapac,[22] a convertible three-dimensional electrostatic code, simulated CHAWS collection with H^+ and O^+ combined for a limited number of trials. The results are included in Table 3 and demonstrate that H^+ may be a significant source of high-voltage current if present in sufficient quantities.

PIC Simulation

Based on the low end of the IRI-90 prediction and the ~10% ceiling suggested by the ram-side sensor, it was decided to estimate the H^+ density as 5% of the total ambient density for the initial simulations. The ambient density and temperature used were those of sweep 10 (Table 2).

The assumption[23] that ion species independently expand into the wake made unnecessary modification of the code to contain both H^+ and O^+. The modification to the PIC code consisted simply of changing the particle mass to that of H^+ from O^+ and ensuring that both the cell size and timestep remain constant. The results become meaningless once the potential expands into the frontal stream because the composition and density there are not physically representative. However, for the purpose of low-voltage simulation these modifications retained the accuracy and characteristics of the original code.

The simulation was run at potentials of 0, −10, −20, and −50 V. Figure 6 shows the H^+ density and potential structure of the probe for the −50-V trial. The probe collected H^+ from many different directions. The isopotential contours demonstrate that at −50 V the collection sheath was near, but did not enter, the frontal stream. Figure 7 shows a quantitative comparison of the code results to the free flight CHAWS data. Both are linear, and the 5% H^+ estimate places the code results within the range covered by the flight data.

Turn-On Voltage Location

The PIC code predicts linear I-V behavior in both the low- and high-voltage ranges. This is in agreement with both the free flight and grappled low-voltage data and, once secondary electron effects were removed, with the behavior of the high-voltage data. It is, therefore, anticipated that at the onset of frontal stream ion collection there will be a discontinuity in the slope of the I-V characteristic.

A turn-on of −84 V is predicted from the sweep 10 PIC run. The −325-V data curves are of sufficient range and have enough

Table 3 Dynapac H^+ results[22]

Φ_P, V	n_∞, m^{-3}	I, μA no H^+	I, μA 10% H^+
−20	1×10^{11}	0	1.7
−100	1×10^{11}	0.8	12.1
−2000	1×10^{11}	115	144

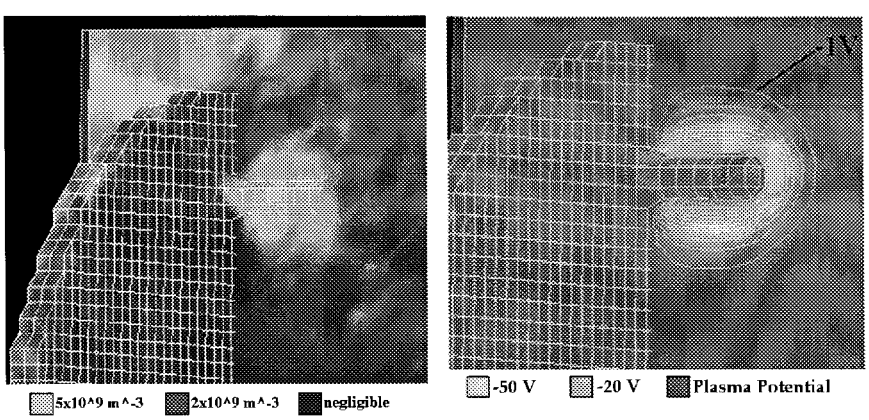

Fig. 6 Centerline cross section of the H^+ ion density (left) and the probe isopotential contours (right).

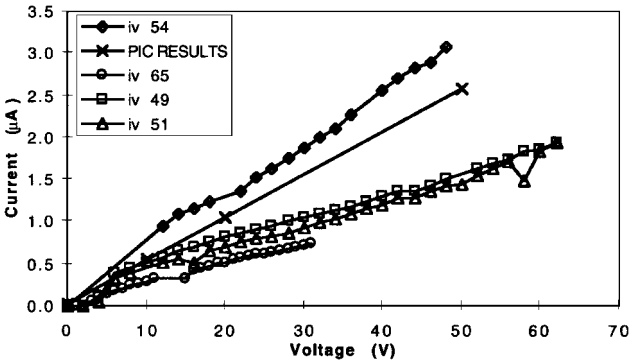

Fig. 7 Comparison of PIC results to free flight data.

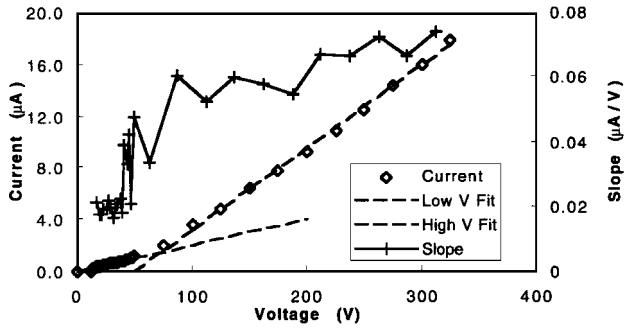

Fig. 8 Example of turn-on voltage location.

low-voltage points that if the turn-on is sharp enough then it should be observable. Examination of these curves in the −50 to −100 V region demonstrates that such a kink exists, as shown in Fig. 8 (sweep 69). The actual turn-on value was determined from the intersection of linear fits to the pre- and postturn-on linear curve segments whereas the error in the value was estimated from the slope vs voltage plot. The values obtained ranged from about −70 to −90 V, increasing slightly with increasing ambient density, and agree with preflight modeling.[5] The error in each value was ±10 V. Preflight CHAWS modeling also predicted that angle of attack would also have a significant effect on the turn-on voltage. Unfortunately, this could not be confirmed because all of the 325-V I-V sweeps were taken at a near zero angle of attack. Turn-on location confirms the code and our understanding that the low- and high-voltage collection regimes differ fundamentally.

Determination of H^+ Density

H^+ was not observed in ram-side sensor measurements.[9] Because an undetected fraction of H^+ can still contribute disproportionately to the current collected, i.e., if H^+ composed 5% of the total ambient density it would be responsible for more than 5% of the probe current (see Table 3), it may be a significant source of error if omitted from the high-voltage simulation, which employed only O^+.

Figure 9 is a plot of probe current vs the measured ambient density at a probe bias of −30 V. The photoemission points are about 0.8 (±0.2) μA above the trend of the sun-shielded points. Each of these points was obtained when the probe was exposing its maximum cross-sectional area to the sun, ~0.046 m^2. The amount of photoemitted current from a stainless-steel surface at 1 AU should be about 20 $\mu A/m^2$ (Ref. 24), and multiplying this by the cross-sectional area predicts that the photocurrent from the probe should be about 0.9 (±0.1) μA. This agreement provides some additional confidence in the described trend, whose slope value is 3.0×10^{-18} $A \cdot m^3$, good to within a factor of about 1.5.

Because Fig. 9 has shown that the low-voltage current scales in a manner proportional to the ambient density the current should also scale proportionately with the ambient H^+ density. An estimate of the current vs H^+ density trend was obtained using the PIC code, and this is also included in Fig. 9. This slope value was 2.3×10^{-18} $A \cdot m^3$ and was given an assumed factor of two error. Dividing the slope values of Fig. 9 shows that the H^+ density was 1.3 (±0.8)%

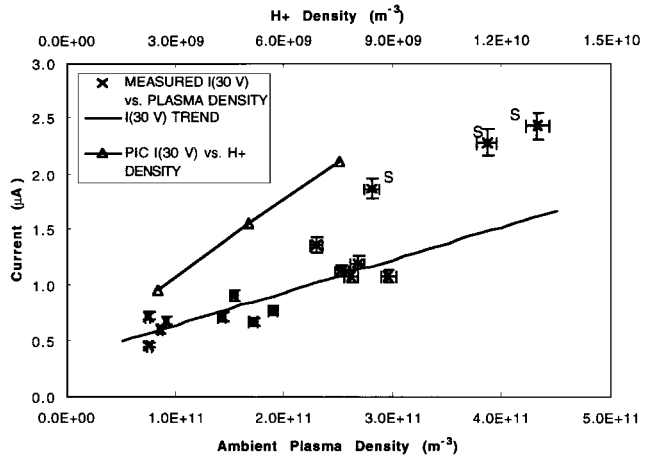

Fig. 9 Measured current vs measured ambient density (×) and PIC H^+ current vs PIC H^+ density (▲) at −30-V probe potential. Points with the S annotation were taken with sunlight directly incident on the probe.

of ambient. As shown by Table 3, if 10% of the frontal stream were H^+, then current would increase by ~25% at −2000 V. Hence, even the maximum allowable value of the derived H^+ density, 2.5%, relegates H^+ to a less than 10% effect at high end voltages. Thus, low Mach number flow cannot be responsible for the high-voltage code–data discrepancy (Fig. 5), and there is no need to include it in the high-voltage simulation.

Ram-Oriented Ion Collection Simulation and Analysis

The CHAWS II flight performed four voltage sweeps with the probe aligned directly into the plasma stream. Three of these sweeps were 300 V in magnitude whereas the fourth was of only 32 V. The ion collection to the probe in this orientation, with $\lambda_D \sim 0.05$ m and $e|(\Phi_P|/kT \gg 1$, was clearly space charged limited. Because the understanding of this collection regime is reasonably comprehensive, this analysis offered the opportunity to employ relevant bodies of work to independently assess the ion density measurements of the ram-side sensors.

Space Charge Collection

Typically the ratio of the electron to ion temperature in an undisturbed LEO plasma is about two. This precludes the work by Bernstein and Rabinowitz[25] and also by Allen et al.[26] because they assumed that electron temperature is much greater than the ion temperature. The more sophisticated work undertaken by Laframboise,[27] which allows for lower electron–ion temperature ratios, is the most applicable to the CHAWS ram-oriented data.

Laframboise[27] extended the Bernstein and Rabinowitz[25] formulation to the physically more reasonable case of a ion Maxwellian distribution. He performed extensive numerical computations for the ion current collection to both spherical and cylindrical probes over a wide range of debye ratio $\xi_P = R/\lambda_D$, temperature ratio $\varepsilon = T_i/T_e$, and probe potential. These calculations are sufficient for determining the current–voltage characteristics of spherical and cylindrical probes over essentially the entire range of practical operation conditions in the collisionless limit. This work employed the Peterson and Talbot[28] fit (good to within 3%) to the numerical results of Laframboise.

Laframboise used a probe that had infinite length. A finite length probe I-V characteristic is affected by the end. This end effect can, as shown by Lederman et al.,[29] increase the observed current several times above that found for probes of effectively infinite length. The proportion of the total current found due to the end effect increases with the $(l_p/r_p)^{-1}$ and the sheath size. Probes with l_p/r_p ratios below about 100–300 may be susceptible depending on the plasma parameters and the Φ_P employed. The CHAWS probe has an l_p/r_p of only 9 and is, therefore, a likely candidate for end effect collection.

Ambient Parameter Estimation

Because the ram-side sensor was oriented into the wake when the shield was inverted there were no direct ambient parameter

measurements available for the ram sweeps. Hence, to allow at least a qualitative comparison of the simulation and the data, estimation of these parameters was necessary.

Figure 10 shows the predicted IRI-90 ion densities compared to the last ion densities measured before the WSF was inverted. Because the terminator advances across the Earth by one orbital period, for each Shuttle orbit the plasma density period is the sum of an orbital period plus the time it takes the Shuttle to travel the distance that the terminator moved (about 10 min). The period of the plasma density is indicated by the two vertical lines in Fig. 10. The IRI-90 prediction and the detector data are in qualitative agreement: each has the largest peak at local midday and subpeaks at local midnight. However, the detector data are consistently below that of the IRI-90 model. The periodicity of the CHAWS density data is the key to estimating the ambient plasma density for sweeps 113–116.

The ram-oriented I-V sweeps were taken almost one orbit following the last ion density measurements. Hence a simple linear extrapolation of the last density measurements is not sufficient to render a density estimate. Rather, it would be more prudent to use density values located one density period prior to the time of the ram sweeps. Becasue the density measurements were continuous for more than one orbit it was possible to leap frog back another density period and obtain an even earlier value for the density. The density value one period prior to the ram sweeps was taken as the actual density estimate whereas the even earlier density value was used to estimate the uncertainty of this method, which was about ±50%. The ion temperature, although not as periodic as the density, was estimated through the same technique. Table 4 displays the estimated values. An estimate of the true electron–ion temperature ratio could not be obtained using the CHAWS ram-side sensor. This was not significant to the wake-side collection but should be important to the space charge limited ram-oriented collection.

Ram-Oriented Simulation

The modifications made to the original high-voltage wake-oriented ion collection code were relatively simple. The flow direction was reversed, all surfaces and boundaries were kept fully accommodating, and the particles were loaded at the opposite side of the simulation. The presence of the shield behind the plate should have only a small effect for WSF potential below a few volts positive. Figure 11 presents the probe ion density profile for −20, −100, and −300 V, as found for sweep 115 density and temperature values under an assumed ε^{-1} of 1.5.

In the −20-V case, the collection sheath was cylindrical around the half of the probe closest to the shield and tapered off toward the tip. In both the −100- and −300-V cases, the sheath was clearly not cylindrical but rather hemispherical.

These findings are consistent with a probe that is suffering from significant end effect. The CHAWS probe, with its low l_p/r_p ratio, was acting almost exclusively as an end at the higher voltages. In the −20-V simulation, the sheath appeared to be at least partially cylindrical indicating that the end effect may not have been as severe at the lower voltages, and this is consistent with the findings of Lederman et al.[29] Figure 12 compares the current found by the experiment, the PIC predicted current, and the Laframboise predicted current. Also included is the current found by a simulation run at −300 V for an ion temperature of 0.14 eV, resulting in slightly decreased current from that found for $T_i = 0.09$ eV.

Because the probe biases were too low for significant emission of negative charge from the probe[12] the difference between the data and the code must be due to error in the ambient parameter code inputs. The uncertainty in the ion density estimation in Table 4 was ±50% but this uncertainty is itself quite uncertain. To determine whether density alone may provide a reasonable explanation for the difference, the code was run at −300 V for a density twice that initially employed. The resulting current is also displayed in Fig. 12 and shows that, although much of the gap was closed, the code and data are still not in good agreement.

A combination of increased density and the electron temperature, however, may be sufficient to match the code and the data. Unfortunately, performing a two-parameter fit between the PIC code and the data would require an inordinate amount of time and computational resource. An alternate method is offered through consideration of the Laframboise[27] results.

The difference between the PIC code prediction and Laframboise's work for the same input parameters should be solely the end effect current. The dominant parameters determining the amount of the end effect are l_p/r_p and Φ_P. Hence, to a first approximation, the factor by which the code is greater than Laframboise prediction at a given voltage, $f_{\text{end}}(\Phi_p)$, are the same for situations of similar ion density and electron temperature. Hence, it should be possible to correct the data for end effect by reducing it by $f_{\text{end}}(\Phi_p)$, assuming

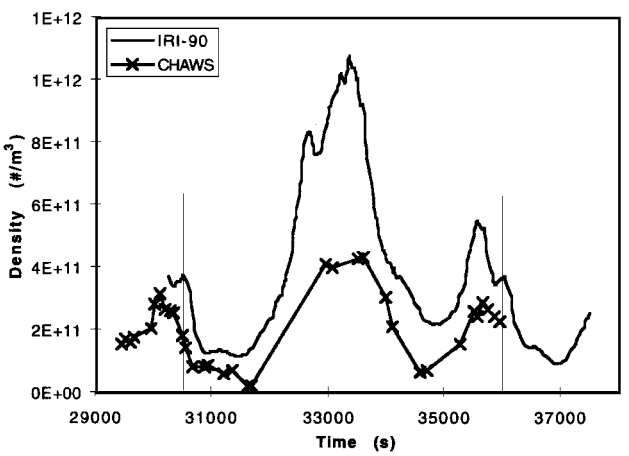

Fig. 10 Comparison of IRI-90 prediction to CHAWS ion density measurements.

Table 4 Estimated ambient parameters for the ram-oriented sweeps

Sweep	Time (universal time), s	Est. n_∞, 10^{10} m^{-3}	Est. T_i, eV
113	40,230	6.5	0.11
114	40,334	8.0	0.11
115	40,482	10	0.09
116	40,616	12	0.09

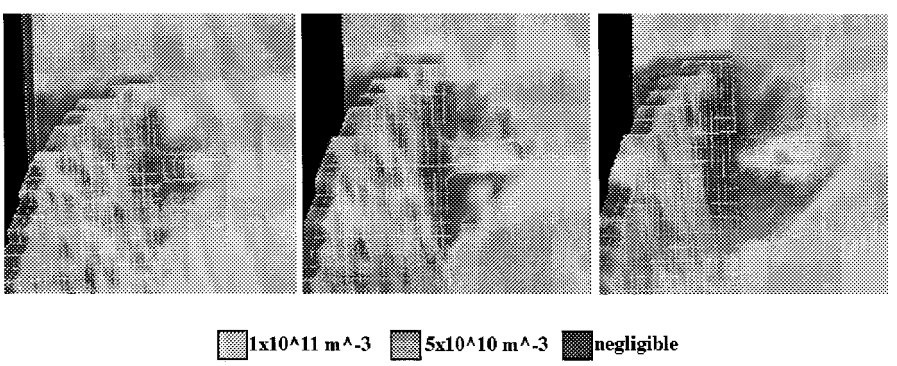

Fig. 11 Ram-oriented PIC ion density profiles for a Φ_P of −20V (left), −100 V (center), and −300 V (right).

Table 5 Summary of high-voltage ion collection simulation uncertainties

Parameter	Error	Impact on I_{PIC}
n_∞	Possibly −33% to −300%	15–170% increase
T_i	±30%	±∼15%
T_e	∼1.5–5T_i	0–10% increase
H^+	——	5–10% increase

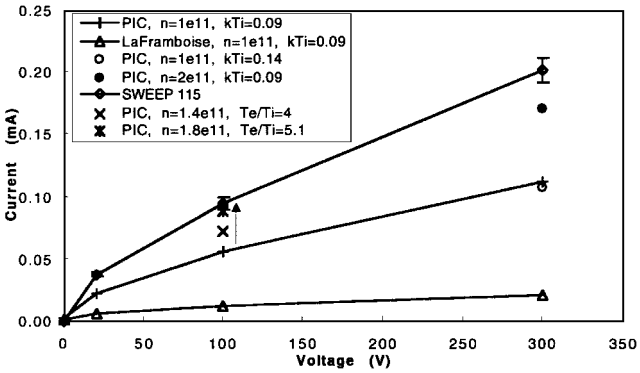

Fig. 12 Comparison of the current–voltage characteristics of the CHAWS ram-oriented sweeps, the PIC simulation, and Laframboise theory.

the density and ion temperature values used to derive $f_{end}(\Phi_p)$ are not significantly different from those of the plasma when the sweep was taken. Once the data were corrected for end effect current, the next iteration ion density and electron–ion temperature ratio could be found by fitting the Laframboise results to it. The new parameters would differ somewhat from those used to generate $f_{end}(\Phi_p)$. Hence, it was necessary to redetermine $f_{end}(\Phi_p)$ for the new ambient parameters by running the code at the new density and temperature values. Therefore, the process for determining the electron–ion temperature ratio and the ion density was iterative but convergent.

The convergence of the PIC code current prediction and sweep 115 is also shown in Fig. 12 by the arrow for −100 V. Similar results were found for sweeps 113 and 116, and they are sufficient to provide two key observations. First, the n_∞ values estimated from the CHAWS detector measurements differ from the obtained fit results by almost a factor of two, more than the ±50% error of the estimate in Table 4. This indicates that the detectors were underestimating the true amount of ion density present by at least one-third or by as much as a factor of 3. This is consistent with the IRI comparison made in Fig. 10 where the CHAWS measured n_∞ is below the IRI-90 prediction by a factor of about 1.5–2.5. An increase in the ion density input to the code by a factor of 2–3 in the high-voltage analysis along with the other smaller errors (refer to Table 5) is sufficient to explain the high-voltage code–data difference.

The second observation provided by the convergence of the ram-oriented simulation and experimental data is that the electron–ion temperature ratio in the disturbed plasma was about two or three times greater than that estimated for an undisturbed plasma. Samir,[30] in his review of plasma disturbances caused by the Space Shuttle and small satellites, states that it is quite clear that the electron temperature behavior in the wake- and ram-side of satellites is a controversial subject. He believes that it is not clear under which plasma and body conditions the temperature enhancement may occur and that it is not obvious whether it is a universal phenomenon or one which is limited to certain types of spacecraft. He suggests that a series of laboratory and in situ experiments be performed to better understand the phenomenon and says that ideal in situ candidates are free fliers and tethered satellites. The results of this analysis suggest that a ram-oriented stainless steel Langmuir probe mounted onto a flat stainless steel disk operating in LEO on the Shuttle robotic arm may observe electron heating. It could not be determined that this heating also occurred in the wake because electron temperature was not measured, and both modeling and analysis[12] show that the wake-oriented ion collection to the probe is insensitive to electron temperature.

Conclusions

The PIC code successfully modeled the main aspects of the CHAWS data and was also able to provide insight that would not have been possible to obtain with the experiment alone. The most notable of the PIC contributions was its ability to be combined with other data analysis (low voltage and ram oriented) to investigate possible reasons for the high-voltage wake-side code–data disagreement. These uncertainties and their estimated impact on the computed current are summarized in Table 5. The reconciliation of the PIC code and the high-voltage ion collection has allowed additional work[12] to develop a general model that allows spacecraft to be designed to better avoid hazardous high-voltage wake charging interactions.

References

[1]Katz, I., and Parks, D. E., "Space Shuttle Orbiter Charging," *Journal of Spacecraft and Rockets*, Vol. 20, No. 1, 1983, pp. 22–25.

[2]Anderson, P. C., and Koons, H. C., "Spacecraft Charging Anomaly on a Low-Altitude Satellite in an Aurora," *Journal of Spacecraft and Rockets*, Vol. 33, No. 5, 1996, pp. 734–738.

[3]Rosen, A., "Spacecraft Charging by Magnetospheric Plasmas," Vol. 47, Progress in Astronautics and Aeronautics, AIAA, New York, 1976.

[4]Svenes, R., and Troim, J., "Laboratory Simulation of Vehicle-Plasma Interaction in LEO," *Planetary and Space Science*, Vol. 42, No. 1, 1994, pp. 81–94.

[5]Cooke, D. L., Talbot, J., and Shaw, G. B., "Pre-Flight POLAR Code Predictions for the CHAWS Space Flight Experiment," U.S. Air Force Phillips Lab., TR PL-TR-94-2056, Hanscom AFB, MA, 1994.

[6]Biasca, R., and Wang, J., "Ion Current Collection in Spacecraft Wakes," *Physics of Plasmas*, Vol. 2, No. 1, 1995, pp. 280–288.

[7]Wang, J., Leung, P., Garrett, H., and Murphy, G., "Multibody–Plasma Interactions: Charging in the Wake," *Journal of Spacecraft and Rockets*, Vol. 31, No. 5, 1994, pp. 889–894.

[8]Enloe, C. L., Cooke, D. L., Meassick, S., Chan, C., and Tautz, M. F., "Ion Collection in a Spacecraft Wake—Laboratory Simulation," *Journal of Geophysical Research*, Vol. 98, No. A8, 1993, pp. 13,635–13,644.

[9]Enloe, C. L., Cooke, D. L., Pakula, W. A., Violet, M. D., Hardy, D., Chaplin, C. B., Kirkwood, R., Tautz, M. F., Bonito, N., Roth, C., Courtney, G., Davis, V. A., Mandell, M. J., Hastings, D. E., Shaw, G. B., Giffin, G., and Sega, R. M., "High-Voltage Interactions in Plasma Wakes: Results from the Charging Hazards and Wake Studies (CHAWS) Flight Experiments," *Journal of Geophysical Research*, Vol. 102, No. A1, 1997, pp. 425–433.

[10]Tribble, A. C., Pickett, J. S., D'Angelo, N., and Murphy, G. B., "Plasma Density, Temperature, and Turbulence in the Wake of the Shuttle Orbiter," *Planetary and Space Science*, Vol. 37, No. 8, 1989, pp. 1001–1010.

[11]Tribble, A. C., D'Angelo, N., Murphy, G., Pickett, J., and Steinberg, J. T., "Exposed High-Voltage Source Effect on the Potential of an Ionospheric Satellite," *Journal of Spacecraft and Rockets*, Vol. 25, 1988, pp. 64–69.

[12]Giffin, G. B., Hastings, D. E., Shaw, G. B., Cooke, D. L., and Enloe, C. L., "A General Model for Use in LEO High Voltage Spacecraft Wake Engineering" (submitted for publication).

[13]Giffin, G. B., "Analysis of the Ion Current Collection in the Plasma Wake During the Charging Hazards and Wake Studies Experiment," M.S. Thesis, Aeronautics and Astronautics Dept., Massachusetts Inst. of Technology, Cambridge, MA, Dec. 1996.

[14]Cooke, D. L., Enloe, C. L., Pakula, W. A., Violet, M. D., Tautz, M. F., Roth, C., Bonito, N., Giffin, G. B., and Shaw, G. B., "Current Voltage Data from the CHAWS Space Flight Experiment," U.S. Air Force Phillips Lab., PL-TR-97-2066, Hanscom AFB, MA, Feb. 1997.

[15]Font, G. I., Hastings, D. E., and Cooke, D. L., "Transient Beam Phenomena Due to Spacecraft Charging in the CHAWS Experiment," AIAA Paper 95-0490, Jan. 1995.

[16]Lilley, J. R., Jr., Cooke, D. L., Jongeward, G. A., and Katz, I., "POLAR Users Manual," U.S. Air Force Phillips Lab., AFGL-TR-89-0307, Hanscom AFB, MA, Feb. 1985.

[17]Shaw, G. B., "Analysis of the Ion Current Collection in the Plasma Wake During the Charging Hazards and Wake Studies Experiment," M.S. Thesis, Aeronautics and Astronautics Dept., Massachusetts Inst. of Technology, Cambridge, MA, June 1995.

[18]Chung, P. M., Talbot, L., and Touryan, K. J., *Electric Probes in Stationary and Flowing Plasmas*, Springer–Verlag, New York, 1975, p. 35.

[19]Singh, N., Samir, U., Wright, K. H., and Stone, N. H., "A Possible Explanation of the Electron Temperature Enhancement in the Wake of a Satellite," *Journal of Geophysical Research*, Vol. 92, 1987, pp. 6100–6106.

[20]Samir, U., Brace, L. H., and Brinton, H. C., "About the Influence of Electron Temperature and Relative Ionic Composition on Ion Depletion in the Wake of the AE-C Satellite," *Geophysical Research Letters*, Vol. 6, 1979, pp. 101–104.

[21]Samir, U., and Kaufman, Y. J., "An Assessment of the Relative Importance of Body and Plasma Properties in Determining the Ion Current Distribution in the Wake of an Ionospheric Satellite," *Journal of Atmospheric and Terrestrial Physics*, Vol. 42, 1980, pp. 533–543.

[22]Mandell, M. J., Davis, V. A., Cooke, D. L., Voilet, M. D., and Enloe, C. L., "CHAWS Wake Side Current Measurements: Comparison with Preflight Predictions," AIAA Paper 95-0489, Jan. 1995.

[23]Samir, U., Comfort, R. H., Chappell, C. R., and Stone, N. H., "Observations of Low-Energy Ions in the Wake of a Magnetospheric Satellite," *Journal of Geophysical Research*, Vol. A5, 1986, pp. 5725–5736.

[24]Hastings, D., and Garrett, H., *Spacecraft Environment Interactions*, Cambridge Univ. Press, New York, 1996.

[25]Bernstein, I. B., and Rabinowitz, I., "Theory of Electrostatic Probes in Low Density Plasma," *Physics of Fluids*, Vol. 2, 1959, pp. 112–121.

[26]Allen, J., Boyd, R. L. F., and Reynolds, P., "The Collection of Positive Ions by a Probe Immersed in a Plasma," *Proceedings of the Physical Society, London, Section B*, Vol. 70, 1957, pp. 297–304.

[27]Laframboise, J. G., Univ. of Toronto Inst. of Aerospace Studies, Rept. 100, Toronto, ON, Canada, 1966.

[28]Peterson, E. W., and Talbot, L., "Collisionless Electrostatic Single-Probe and Double-Probe Measurements," *AIAA Journal*, Vol. 8, No. 12, 1970, pp. 2215–2219.

[29]Lederman, S., Bloom, M. H., and Widhopf, G. F., "Experiments on Cylindrical Electrostatic Probes in a Slightly Ionized Hypersonic Flow," *AIAA Journal*, Vol. 6, No. 11, 1968, pp. 2133–2139.

[30]Samir, U., Stone, N. H., and Wright, K. H., "On Plasma Disturbances Caused by the Motion of the Space Shuttle and Small Satellites: A Comparison of In Situ Observations," *Journal of Geophysical Research*, Vol. 91, 1986, pp. 277–285.

A. C. Tribble
Associate Editor